MOL PHARM

MOLECULAR PHARMACOLOGY

Function of Both Sinusoidal and Canalicular Transporters Controls the Concentration of Organic Anions within Hepatocytes

Corinne Planchamp, Antoine Hadengue, Bruno Stieger, Joëlle Bourquin, Alain Vonlaufen, Jean-Louis Frossard, Rafael Quadri, Christoph D. Becker, and Catherine M. Pastor

Laboratoire de Physiopathologie Hépatique et Imagerie Moléculaire (C.P., J.B., C.M.P.); Division de Gastroentérologie et Hépatologie (A.H., A.V., J.L.F., R.Q.); and Département de Radiologie, Hôpitaux Universitaires de Genève, Geneva, Switzerland (C.D.B.); and Klinische Pharmakologie und Toxicologie, UniversitätsSpital Zürich, Zurich, Switzerland (B.S.)

ABSTRACT

We hypothesized that the function of both sinusoidal and canalicular transporters importantly controls the concentrations of organic anions within normal hepatocytes. Consequently, we investigated how acute transport regulation of the sinusoidal organic anion transporting polypeptides (Oatps) and the canalicular multidrug resistance associated protein 2 (Mrp$_2$) determines the hepatic concentrations of the organic anion gadolinium benzyloxypropionictetraacetate (BOPTA) in rat livers. Livers were perfused with labeled BOPTA in different experimental settings that modify the function of Oatps and Mrp$_2$ through the protein kinase C (PKC) pathway. Intrahepatic concentrations were continuously measured with a gamma probe placed above rat livers. Labeled BOPTA was also measured in perfusate and bile. We showed that when the function of Oatps and Mrp$_2$ is modified in such a way that BOPTA entry and exit are similarly decreased, concentrations of organic anions within hepatocytes remain unaltered. When exit through Mrp$_2$ is abolished, hepatic concentrations are high if entry through Oatps is only slightly decreased (livers without Mrp$_2$ expression) or low if BOPTA uptake is more importantly decreased (livers perfused with a PKC activator). These results highlight that the function of both sinusoidal and canalicular transporters is important to determine the concentration of organic anions within hepatocytes.

One of the major functions of the liver is to detoxify endogenous and exogenous compounds that are eliminated into bile. The overall transport of these compounds across hepatocytes is supported by transporters located on the sinusoidal and canalicular membranes (Meier et al., 1997; Kullak-Ublick et al., 2000). Among these compounds, organic anions are taken up by the organic anion transporting polypeptide (OATP/SLC21A) family of proteins (Hsiang et al., 1999; König et al., 2000; Kullak-Ublick et al., 2001; Cui et al., 2003) and excreted into bile via the ATP-binding cassette transmembrane transporters, multidrug resistance associated protein 2 (MRP$_2$/ABCC$_2$) (Keppler and König, 1997).

The overall transport of organic anions through hepatocytes is difficult to assess because methods that investigate the uptake of organic anions differ from those used to measure bile export and because most organic anions are metabolized within hepatocytes, the biliary compound being different from the compound that had entered through the sinusoidal membrane. However, efforts to quantify the overall transport through both transporters in Madin-Darby canine kidney II cells that were transfected with both Oatps and Mrp$_2$ transporters have been recently described (Sasaki et al., 2004; Matsushima et al., 2005).

Another way to investigate the overall transport of organic anions is to measure the transport of labeled compounds in perfused rat livers as described previously (Patel et al., 2003; Hoffmaster et al., 2004; Chandra et al., 2005). In a similar experimental model, we recently perfused the magnetic resonance imaging (MRI) contrast agent gadolinium benzyloxypropionictetraacetate (BOPTA; MultiHance, Bracco Diagnostics, Princeton, NJ) labeled with [153]Gd and measured

ABBREVIATIONS: OATP, organic anion transporting polypeptide; MRI, magnetic resonance imaging; BOPTA, gadolinium benzyloxypropionictetraacetate; KHB, Krebs-Henseleit-bicarbonate; ZO, zona occludens; HRP, horseradish peroxidase; PKC, protein kinase C; PMA, phorbol 12-myristate 13-acetate; E3S, estrone-3-sulfate; DTPA, gadolinium diethylenetriaminepentaacetic acid; ANOVA, analysis of variance; Gö6976, 12-(2-cyanoethyl)-6,7,12,13-tetrahydro-13-methyl-5-oxo-5H-indolo(2,3-a)pyrrolo(3,4-c)-carbazole; BSP, bromosulfophthalein; VP, vasopressin.

the radioactivity of this organic anion in perfusate and bile samples, as well as within the liver using a gamma scintillation probe placed above the liver (Planchamp et al., 2005b). A six-compartment pharmacokinetic model describes BOPTA transport in the entire liver, and BOPTA entry into hepatocytes and exit are estimated by rate constants.

In liver imaging, BOPTA facilitates the detection and characterization of hepatic tumors. Because BOPTA is an organic anion, the compound enters into hepatocytes through members of the Oatp family and exits without biotransformation into bile through Mrp$_2$. As expected, BOPTA uptake in perfused rat livers is inhibited by the coadministration of bromosulfophthalein (Pastor et al., 2003). We showed that BOPTA-induced hyperintensity in liver imaging (or intrahepatic concentration) was similar in cirrhotic and normal rat livers although Mrp$_2$ and Oatp expression was markedly down-regulated by cirrhosis (Planchamp et al., 2005a). Thus, in liver imaging, hyperintensity induced by intrahepatic BOPTA concentration was not correlated to the expression of Oatps and Mrp$_2$. Consequently, one explanation might be that BOPTA is trapped into cirrhotic livers when biliary excretion through Mrp$_2$ is abolished, preventing liver imaging from differentiating between normal livers and those affected by a pathological condition.

The aim of our study was to determine how acute regulation of Oatps and Mrp$_2$ determines the hepatic concentrations of labeled BOPTA. In normal perfused livers, transport through Oatps and Mrp$_2$ was differently modified through the protein kinase C pathway, and we determined the consequences of such modifications on intracellular BOPTA concentrations.

Materials and Methods

Animals

Before liver perfusion, normal Sprague-Dawley rats (250–450 g) were anesthetized with pentobarbital (50 mg/kg i.p.). The protocol was approved by the animal welfare committee of the University of Geneva and the veterinary office and followed the guidelines for the care and use of laboratory animals.

Rat Liver Perfusion

Livers were perfused in situ as described previously (Pastor et al., 1996). In brief, the abdominal cavity was opened, and the portal vein was cannulated and secured. A 16-gauge catheter (outer diameter, 1.8 mm) was introduced into the portal vein up to 2 to 3 mm from the liver. A ligature was placed around the inferior vena cava above the left renal vein. After the cannulation of the portal vein, the abdominal vena cava was transected, and the Krebs-Henseleit-bicarbonate (KHB) solution (118 mM NaCl, 1.2 mM MgSO$_4$, 1.2 mM KH$_2$PO$_4$, 4.7 mM KCl, 26 mM NaHCO$_3$, and 2.5 mM CaCl$_2$) was pumped without delay into the portal vein. The flow rate was slowly increased over 1 minute up to 30 ml/min. In a second step, the chest was opened and a second cannula (14-gauge) was inserted through the right atrium into the thoracic inferior vena cava and secured with a ligature. Finally, the ligature around the abdominal inferior vena cava was tightened. The KHB solution was perfused to the liver through the portal catheter and eliminated by the catheter placed in the thoracic inferior vena cava. In each experiment, the common bile duct was cannulated with a PE10 catheter.

The entire perfusion system consisted of reservoir, pump, heating circulator, bubble trap, filter, and oxygenator. The livers were perfused with KHB buffer during the entire protocol with a nonrecirculating perfusion. The perfusate was equilibrated with a mixture of 95% O$_2$/5% CO$_2$ during the protocol.

Quantification of Hepatic BOPTA Transport

BOPTA was labeled by adding ^{153}GdCl$_3$ to a 0.5 M BOPTA solution (1 MBq/ml), which contains a slight excess of ligand BOPTA (Planchamp et al., 2005a,b). The contrast agent was then diluted in KHB solution to obtain a 200 μM perfusion solution. To quantify intrahepatic concentrations of BOPTA, a gamma scintillation probe that measures radioactivity every 20 s was placed 1 cm above the liver (Planchamp et al., 2005b). To transform radioactivity counts into contrast agent amounts, the radioactivity in the entire liver at the end of each experiment was measured (Activimeter Isomed 2000; MCD Nuklear Medizintechnik, Dresden, Germany) and related to the last count measured by the probe. Bile and perfusate samples were collected and radioactivity was measured by a Cobra auto-Gamma counter (PerkinElmer, Rotkreutz, Switzerland). For each experiment, the total amount of radioactivity perfused in each liver was totally recovered at the end of the experiment in perfusate, liver, and bile. The perfusion of ^{153}Gd-BOPTA in normal rat livers was successfully described by a six-compartmental model with a rate constant between the extracellular volume and hepatocytes that estimates BOPTA uptake (k_{uptake}) and a rate constant between hepatocytes and bile that estimates hepatic BOPTA excretion ($k_{excretion}$) (Planchamp et al., 2005b).

Immunofluorescence

Liver biopsies (0.5 cm^2) were embedded in OCT, frozen in isopentane precooled in liquid nitrogen and kept at -20°C until used. Tissue samples were cut (5-μm sections) at -20°C and placed on Superfrost plus slides (Menzel, Braunschweig, Germany). After fixation with pure methanol (-20°C, 15 min), the sections were covered with Triton X-100 [0.1% in phosphate-buffered saline (PBS) for 10 min], washed with PBS, and covered with 1% bovine serum albumin in PBS for 15 min. A mixture of polyclonal rabbit anti-rat Mrp$_2$ antibody (1:500) and monoclonal rat anti-mouse ZO-1 antibody (1:500; Biozol, Eching, Germany) or PBS for control staining was applied for 1 h of incubation in a wet chamber. After rinsing and washing, slides were incubated for 45 min with a mixture of fluorescein isothiocyanate-conjugated goat anti-rabbit IgG (1:100) and TR-conjugated goat anti-rat IgG (1:200) (Jackson ImmunoResearch Laboratories Inc., West Grove, PA). After a final washing, sections were covered with mounting medium and a coverslip. Images were acquired from two channels at wavelengths of 488 nm to visualize Mrp$_2$ and 568 nm to visualize ZO-1 with a confocal laser scanning microscope (Zeiss Axiophot 1; Carl Zeiss GmbH, Jena, Germany) equipped with an Axiocam color CCD camera (Carl Zeiss). Identical settings were used to compare liver sections from different experimental conditions.

Bile HRP Activity

Horseradish peroxidase (HRP; 0.05 mg/ml), which is transported through hepatocytes into vesicles from the sinusoidal to the canalicular membranes, was perfused in the presence or in the absence of BOPTA as described previously (Beuers et al., 1993). Bile HRP activity was measured spectrophotometrically using 4-aminoantipyrine as substrate by recording the linear change in adsorption at 510 nm for 3 min at 25°C. HRP activity was calculated according to a HRP standard curve and expressed as nanograms of protein per minute per gram of liver.

Western Blotting Analysis

To detect cytosolic and membrane PKCα and PKCε, hepatic tissues were homogenized at 4°C in lysis buffer [50 mM Tris-HCl, pH 7.5, 2 mM EGTA, 2 mM EDTA, 50 μg/ml phenylmethylsulfonyl fluoride, 1% protease inhibitor cocktail, and 1% phosphatase inhibitor cocktail I and II (Sigma, St. Louis, MO)] as described previously

(Roelofsen et al., 1991). After sonication, extracts were ultracentrifuged at $100,000g$ for 1 h. The pellet was then extracted with the same buffer containing 1% Triton X-100, sonicated, and ultracentrifuged at $100,000g$ for 20 min. Cytosolic proteins were present in the supernatant of the first centrifugation, and cell membrane-bound proteins were present in the supernatant of the second centrifugation. Protein contents were quantified by the Bradford technique. SDS polyacrylamide gel electrophoresis and Western blotting were performed according to Laemmli using minigels (Bio-Rad Laboratories, Glattbrugg, Switzerland). Protein extracts (50 μg) were separated on a 10% polyacrylamide gel. After the gel had been transferred to a polyvinylidene difluoride membrane (Millipore, Volketswil, Switzerland), the membrane was blocked with 5% nonfat dry milk PBS (1 h at room temperature) and incubated overnight at 4°C with specific antibodies (250 ng/ml; BD Transduction Laboratories, Lexington, KY). The membrane was washed four times in PBS-Tween 20 and incubated for 1 h with an alkaline phosphatase-conjugated secondary antibody. After washing, detection was achieved by chemiluminescence (Immune-Star; Bio-Rad Laboratories) according to the manufacturer's instructions. Molecular weight markers and positive controls were included for each experiment. Films were scanned using an ImageScanner densitometer equipped with the Labscan and ImageQuant software (GE Healthcare, Little Chalfont, Buckinghamshire, UK). Staining with Ponceau Red before blocking assessed that equal quantity of proteins was loaded on each line.

BOPTA Uptake Studies in *Xenopus laevis* Oocytes

In vitro synthesis of Oatp$_1$, Oatp$_2$, and Oatp$_4$ cRNA was performed as described previously (Hagenbuch et al., 1990; Noé et al., 1997). *X. laevis* oocytes were prepared and cultured overnight at 18°C. Healthy oocytes were microinjected with 0.5 ng of Oatp$_1$, Oatp$_2$, or Oatp$_4$ cRNA and cultured for 3 days in a modified Barth solution containing 88 mM NaCl, 2.4 mM NaHCO$_3$, 1 mM KCl, 0.33 mM Ca(NO$_3$)$_2$, 0.41 mM CaCl$_2$, 0.82 mM MgSO$_4$, 100 mg/ml penicillin/streptomycin, and 10 mM HEPES, adjusted to pH 7.5 with 5 M NaOH. The uptake medium included 100 mM NaCl, 2 mM KCl, 1 mM CaCl$_2$, 1 mM MgCl$_2$, and 10 mM HEPES, pH 7.5. Oocytes were prewashed with uptake medium and incubated for 30 min at 25°C in 150 μl of medium in the presence or the absence of the PKC activator phorbol 12-myristate 13-acetate (PMA; 1 μM). Oocytes were then washed in uptake medium and incubated at 25°C in 150 μl of uptake medium with 500 nM [³H]estrone-3-sulfate (E3S), 200 μM ¹⁵³Gd-labeled BOPTA, or 200 μM ¹⁵³Gd-labeled gadolinium diethylenetriaminepentaacetic acid (DTPA, Magnevist; Bayer Schering Pharma AG, West Sussex, UK). Water-injected oocytes were used as controls to detect nonspecific uptake of substrates. Then substrate uptake was stopped by addition of ice-cold uptake medium (6 ml). Oocytes were washed twice with ice-cold uptake medium (6 ml) and the oocyte-associated ¹⁵³Gd-BOPTA and ¹⁵³Gd-DTPA was measured (Cobra Auto-Gamma counter). To determine [³H]E3S uptake, each oocyte was dissolved in 0.25 ml of 10% SDS, and the oocyte-associated radioactivity was measured in a Tri-Carb liquid scintillation analyzer (PerkinElmer Life and Analytical Sciences, Boston, MA) after the addition of 4 ml of scintillation fluid (Ultima Gold; PerkinElmer),

Experimental Groups

Choleretic Effect of BOPTA in Perfused Livers. To study the effect of BOPTA on bile flow and bile excretion, we perfused three livers with 200 μM BOPTA for 30 min (KHB model). BOPTA perfusion was followed by a rinse period with KHB solution (30 min). Control livers ($n = 3$) were perfused with KHB perfusion in the absence of BOPTA during 60 min.

To determine whether the increase in bile flow induced by BOPTA was PKC-dependent, we perfused additional livers with KHB and the nonspecific PKC inhibitor Gö8530 (1 μM, $n = 3$) or KHB + the

Ca²⁺-specific PKC inhibitor Gö6976 (1 μM, $n = 3$) before BOPTA perfusion.

We then determined whether BOPTA perfusion interferes with hepatic vesicular transport by measuring bile HRP excretion in the presence or the absence of BOPTA. In each group, livers were perfused with 0.05 mg/ml HRP or 200 μM BOPTA + 0.05 mg/ml HRP ($n = 3$, in each group).

BOPTA Membrane Transporters. Because the transport of BOPTA through Mrp$_2$ had not been previously demonstrated in isolated livers, we perfused four livers isolated from Mrp$_2$-deficient (TR⁻/⁻) rats with BOPTA. Because bromosulfophthalein (BSP; 200 μM) enters into hepatocytes via Oatps (Hagenbuch and Meier, 2003), we perfused three control livers with BOPTA and BSP to confirm that the contrast agent enters through the same family of transporters as BSP. Moreover, the uptake of BOPTA through Oatps was measured in oocytes infected with the three Oatp cRNAs (Oatp$_1$, Oatp$_2$, and Oatp$_3$) described in rat livers.

Effect of BOPTA in Livers Preperfused with the PKC Activator PMA: the PMA Model. Livers ($n = 3$) were preperfused with 1 μM PMA for 30 min before the perfusion of 200 μM BOPTA (30 min) and the rinse solution with KHB (30 min). To confirm the effect of PMA perfusion on PKC isoforms, we perfused additional livers concomitantly with PMA and either the nonspecific PKC inhibitor Gö8530 (1 μM, $n = 3$) or the Ca²⁺-specific inhibitor Gö6976 (1 μM, $n = 3$). Two other groups were also perfused with Gö8530 or with Gö6976 in the absence of BOPTA to assess the effects of the PKC inhibitors alone.

Effect of BOPTA in Livers Preperfused with Vasopressin: the VP Model. Because PKC isoform activation by PMA is not physiologic, we preperfused livers isolated from normal rats with VP that activates V$_1$ receptor on the sinusoidal membrane of hepatocytes, releasing diacylglycerol, which endogenously activates PKC. VP (10 nM) was perfused during 30 min before the perfusion of BOPTA (30 min) and the rinse solution with KHB (30 min). To confirm the effect of VP perfusion on PKC isoforms, we perfused additional livers with VP and either the nonspecific PKC inhibitor Gö8530 (1 μM, $n = 3$) or the Ca²⁺ specific inhibitor Gö6976 (1 μM, $n = 3$).

Statistics

Values are means ± S.D. Means are compared by a one-way ANOVA and Dunnett test for multiple comparisons or two-way ANOVA.

Results

Choleretic Effect of BOPTA in Perfused Livers. When BOPTA was perfused in normal livers, bile flow importantly increased concomitantly with BOPTA bile excretion (Fig. 1A; $p < 0.0001$) and this choleretic effect was not modified by the preperfusion with Gö6850 (inhibitor of PKC) or Gö6976 (inhibitor of Ca²⁺-dependent PKC). Likewise, BOPTA bile excretion was not modified by the preperfusion with Gö6850 or Gö6976 (Fig. 1B, $p = 0.56$).
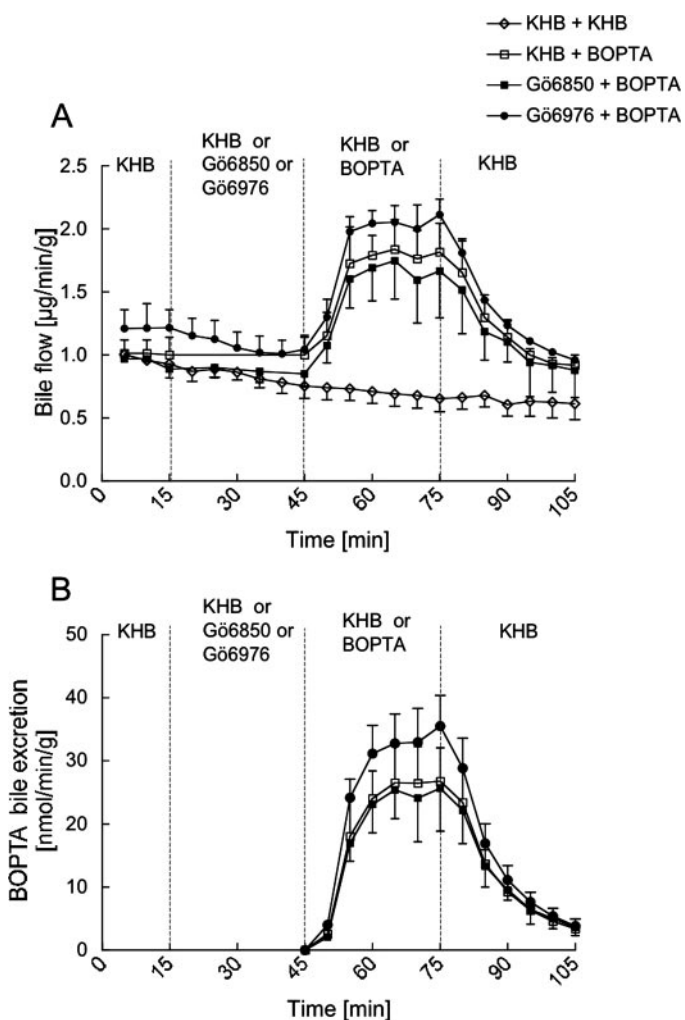
HRP transport within vesicles from the sinusoidal to the canalicular membrane of hepatocytes did not modify BOPTA bile excretion (Fig. 2A; $p = 0.63$) and BOPTA transport did not modify HRP bile excretion (Fig. 2B; $p = 0.79$). Maximal HRP bile excretion occurred later than BOPTA bile excretion, suggesting that BOPTA has a carrier-mediated transport by cytoplasmic proteins rather than a vesicular transport. Bile flow was similar in livers perfused with KHB or HRP solutions, and the choleretic effect of BOPTA was not modified by the addition of HRP (data not shown).

BOPTA Membrane Transporters. In perfused livers, BSP (200 μM) completely inhibited BOPTA entry into the

entire liver (Fig. 3C), confirming that the sinusoidal transporters of BOPTA are Oatps, similar to BSP. The isoforms of Oatps responsible for BOPTA uptake in hepatocytes have never been determined. Consequently, we infected oocytes with the rat cRNA of $Oatp_1$, $Oatp_2$, or $Oatp_4$ (the three Oatps identified in rat livers) and measured the uptake of BOPTA within oocytes. In contrast to the organic anion E3S that mainly entered into oocytes through $Oatp_1$ (and to a lesser extent through $Oatp_4$), BOPTA entered into oocytes through $Oatp_1$, $Oatp_2$, and $Oatp_4$ (Fig. 3, A and B).

In livers isolated from $TR^{-/-}$ rats, we also confirmed that the hepatic canalicular transporter of BOPTA was Mrp_2 (Fig. 3D). When livers from $TR^{-/-}$ rats were perfused with BOPTA, the amount of contrast agent in bile was close to 0 (data not shown). Moreover, BOPTA accumulation in livers was much higher in $TR^{-/-}$ than in normal livers ($p < 0.001$). It is noteworthy that before BOPTA perfusion, bile flow was significantly lower in $TR^{-/-}$ than in normal rats 20 min after the start of hepatic perfusion (0.52 ± 0.18 versus 0.87 ± 0.08 $\mu g/min/g$, respectively). As expected by the absence of BOPTA excretion, bile flow during BOPTA perfusion in $TR^{-/-}$ livers did not increase (data not shown).

Thus, BOPTA is a choleretic organic anion that enters into rat hepatocytes through Oatps and exits unchanged into bile through Mrp_2. The choleretic effect of BOPTA is not PKC-dependent and the intracellular trafficking of the organic anion is mediated by cytoplasmic proteins.

No Choleretic Effect of BOPTA in the PMA Model. To modify the transport through Oatps and Mrp_2, we preperfused livers with PMA that directly activates PKC (PMA model). PMA activated $PKC\alpha$ that migrates in the cellular membrane fraction (Fig. 4). PKC activation was associated with a decrease in bile flow from 1.18 ± 0.17 to 0.18 ± 0.05 $\mu g/min/g$ before and after PMA perfusion, respectively, without recovery overtime ($0.13 + 0.09$ $\mu g/min/g$ at the end of the experiments).

After PMA perfusion, BOPTA had no choleretic effect, and the organic anion was unable to reverse the cholestasis induced by PMA. Coperfusion of PKC inhibitors with PMA prevented the effects of PMA on bile flow (Fig. 5A; $p = 0.003$) and BOPTA maximal bile excretion (Fig. 5B; $p = 0.002$). Thus, BOPTA is a choleretic organic anion in normal livers without anticholestatic effect in our PMA model.

Decreased Choleretic Effect of BOPTA in the VP Model. In additional groups, we preperfused livers isolated from normal rats with VP that activates V_1 receptor on the sinusoidal membrane of hepatocytes, releasing diacylglycerol, which endogenously activates PKC. VP was
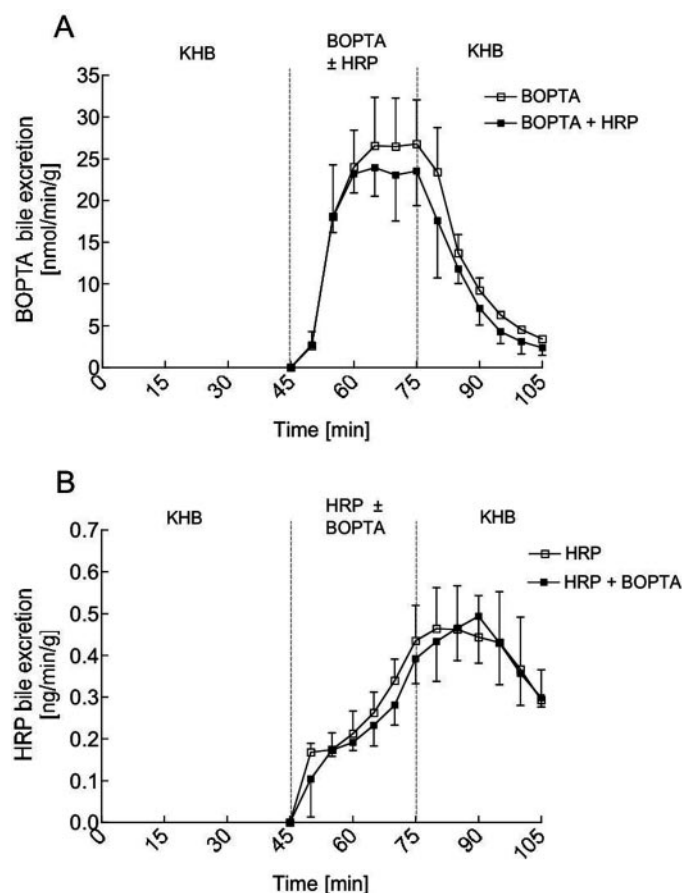

Fig. 1. Bile flow (A) and BOPTA bile excretion (B) in perfused livers during the following perfusion conditions: KHB from 0 to 15 min; KHB, KHB + the nonspecific PKC inhibitor Gö8530 (1 μM), or KHB + the Ca^{2+}-specific PKC inhibitor Gö6976 (1 μM) from 15 to 45 min; BOPTA (200 μM) from 45 to 75 min; and KHB from 75 to 105 min.

Fig. 2. BOPTA bile excretion (A) and HRP bile excretion (B) in perfused livers during the following perfusion conditions: KHB from 0 to 45 min; KHB + BOPTA (200 μM), KHB + BOPTA + HRP (0.05 mg/ml) from 45 to 75 min; KHB from 75 to 105 min.

perfused during 30 min before BOPTA and did not modify bile flow (data not shown) but decreased the choleretic effect of BOPTA compared with livers preperfused with KHB alone (Fig. 5A, $p = 0.03$). BOPTA maximal bile excretion was significantly lower in livers preperfused with VP than in livers preperfused with KHB solution (Fig. 5B, $p = 0.01$). Coperfusion of PKC inhibitors with VP prevented these effects, demonstrating that VP activates PKC via the release of endogenous diacylglycerol (Fig. 5, A and B).

Mrp_2 Localization in the KHB-, PMA-, and VP Models. To investigate the putative mechanism of decreased BOPTA bile excretion in the PMA and VP models, we studied the localization of Mrp_2 in the canalicular membrane by immunofluorescence in the various conditions of perfusion. We first confirmed that $TR^{-/-}$ rats had no Mrp_2 transporters (Fig. 6). In the KHB model, no Mrp_2 could be observed outside the limits of ZO-1 (a tight-junction protein) (Fig. 6). In

contrast, in the VP and PMA models, Mrp_2 was detected outside the ZO-1 limits during BOPTA perfusion.

Estimation of BOPTA Uptake and Exit in Entire Livers. In entire livers, BOPTA transport was estimated by the rate constants k_{uptake} and $k_{excretion}$ (Table 1). k_{uptake} was significantly lower in the PMA model than in the KHB model, whereas $k_{excretion}$ was abolished in the PMA model and $TR^{-/-}$ liver and significantly decreased in the VP model. Concomitant perfusion of PMA and VP with Gö6850 or Gö6976 prevented the modifications of k_{uptake} and $k_{excretion}$ induced by PMA and VP alone.

Intrahepatic Concentrations of BOPTA. Modifications of BOPTA transport through Oatps and Mrp_2 in the PMA model decreased the intrahepatic accumulation of BOPTA within the liver (Fig. 7, $p < 0.005$). BOPTA hepatic accumulation was similar in the VP and KHB models. Coperfusion of PKC inhibitors with PMA prevented the decreased BOPTA accumulation (data not shown).
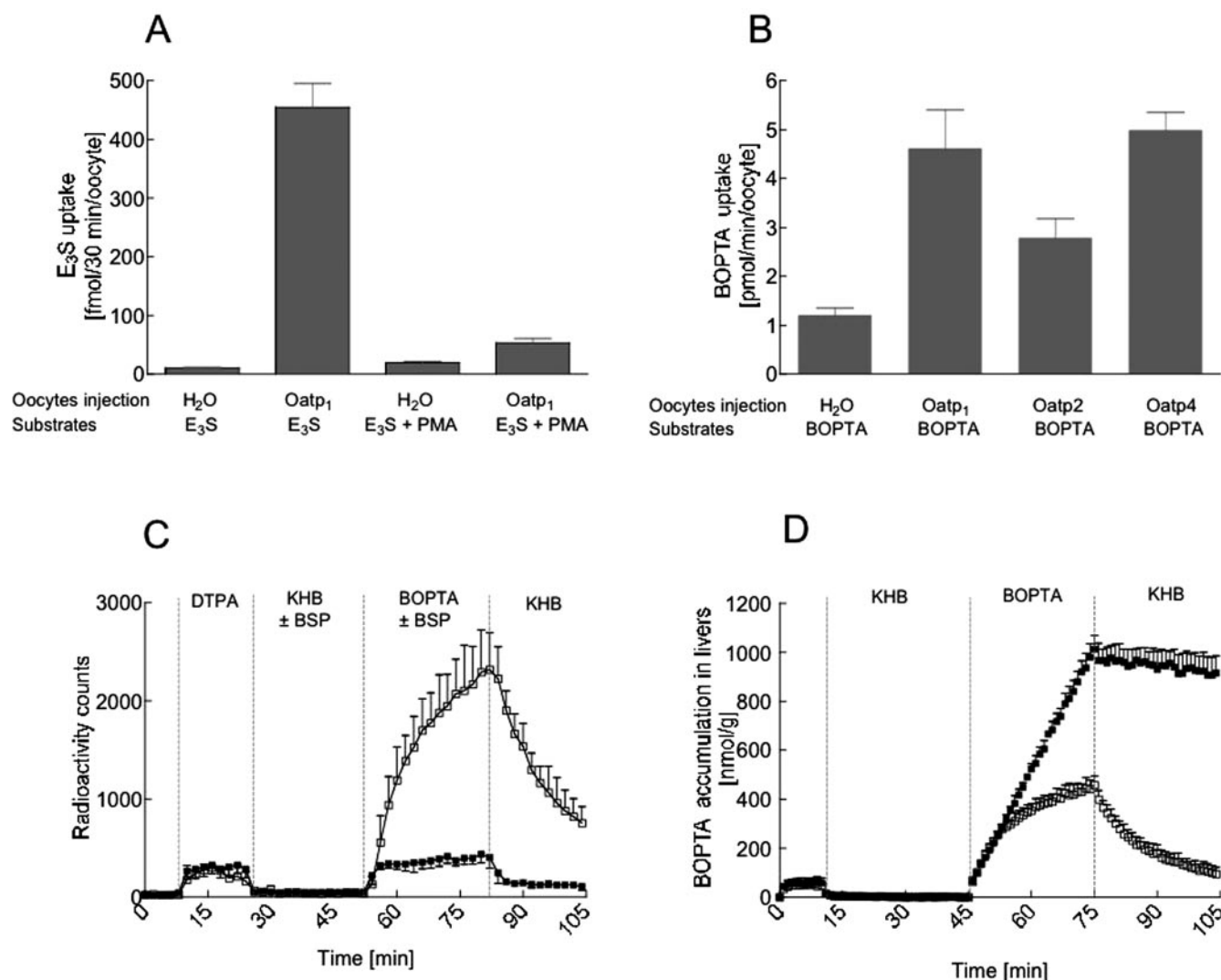
Fig. 3. Uptake of [³H]E3S (A) and ¹⁵³Gd-labeled BOPTA (B) in healthy oocytes. Oocytes were microinjected with the cRNA of $Oatp_1$, $Oatp_2$, and $Oatp_4$, cultured for 3 days, and incubated in uptake medium with E3S (500 nM) or BOPTA (200 μM). Water-injected oocytes were used as controls to detect nonspecific uptake of substrates. E3S uptake was measured in the presence or the absence of the PKC activator PMA (1 μM). $n = 10–19$ oocytes in each group (A and B). Accumulation of BOPTA and DTPA (extracellular contrast agent) into the livers measured by the gamma scintillation probe placed above the livers (C and D). Livers were perfused with 200 μM DTPA and KHB for 30 min, 200 μM BOPTA ± 200 μM BSP for 30 min, and KHB. C, normal livers were perfused with BOPTA (□) or BOPTA + BSP (■). D, livers isolated from normal rats (□) or $TR^{-/-}$ rats (■) were perfused. No radioactivity was measured in bile during the perfusion of the extracellular contrast agent DTPA. Data are mean ± S.D.

Discussion

The contrast agent BOPTA has been developed to facilitate the detection and characterization of hepatic tumors by MRI. After BOPTA injection, early dynamic images obtained during arterial, portal, and interstitial phases are useful to characterize focal lesions. Acquisition of delayed images also increases the potential for lesion detection (Manfredi et al., 1998; Grazioli et al., 2001). With these late images, BOPTA associates nonspecific extracellular distribution with intra-hepatocyte accumulation, as well as possible retention in bile canaliculus, the role of BOPTA concentrations within hepatocytes being the greatest contributor to signal intensities at this phase. We have reported intriguing results showing that BOPTA-induced hyperintensity in liver imaging was similar in cirrhotic and healthy livers, although Mrp_2 and Oatps expression was markedly down-regulated by cirrhosis (Planchamp et al., 2005a). Consequently, one explanation might be that BOPTA is trapped into cirrhotic livers when biliary excretion through Mrp_2 is abolished, preventing liver imaging from differentiating between normal livers and those affected by a pathological condition. We then hypothesized that intracellular concentrations of BOPTA are importantly controlled by the function of Oatps and Mrp_2.

In the present study, we show that concentrations of BOPTA within hepatocytes are highly dependent on the function of both sinusoidal and canalicular transporters that mediate entry and exit of the compound. When PKC activation by VP modulates both Oatps and Mrp_2 function in such a way that BOPTA entry and exit are similarly decreased, concentrations of organic anions within hepatocytes remain unaltered. When exit through Mrp_2 is abolished ($TR^{-/-}$ rats or PMA model), hepatic concentrations are high if entry through Oatps is slightly decreased ($TR^{-/-}$ rats) or low if BOPTA uptake is more importantly decreased (PMA model). These results highlight that the function of both sinusoidal and canalicular transporters is important to determine the concentrations of organic anions within hepatocytes.

BOPTA Transport through Hepatocytes. As with other organic anions, we showed that BOPTA enters into hepatocytes through Oatps. In perfused livers, BOPTA entry into hepatocytes was abolished by the coperfusion of BSP (another organic anion that enters through Oatps into hepatocytes) and, in the presence of BSP, BOPTA behaves similarly to the well known extracellular contrast agent DTPA (Fig. 3C). Moreover, no BOPTA is detected in bile samples during the coperfusion of BOPTA and BSP. In a similar experimental model, we previously showed by hepatic MRI that BSP totally abolishes the signal intensity enhancement induced by the coperfusion of BOPTA and BSP (Pastor et al., 2003). In isolated hepatocytes, we confirmed the cellular entry of BOPTA through a membrane transporter that is saturable at high substrate concentrations with a K_m of 270 ± 111 μM and a V_{max} value of 6.62 ± 1.38 SI units at 30 min (Planchamp et al., 2004). Three Oatps have been described in rat livers: $Oatp_1$, $Oatp_2$, and $Oapt_4$ (Hagenbuch and Meier, 2003). Consequently, the cRNA of $Oatp_1$, $Oatp_2$, or $Oatp_4$ were microinjected in healthy oocytes, and we showed that BOPTA was mainly taken up by $Oatp_1$ and $Oatp_4$. Van Montfoort et al. (1999) showed that gadolinium ethoxybenzyl diethylenetriaminepentaacetic acid (another hepatospecific contrast agent close to BOPTA) is taken up in healthy oocytes by $Oatp_1$ but not $Oatp_2$. Uptake of gadolin-
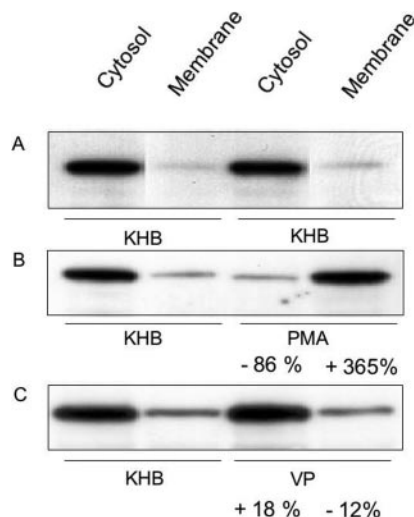
Fig. 4. $PKC\alpha$ expression in cytosol or membrane in biopsies collected from the same livers during various conditions of perfusion: A, KHB solution for 30 min and KHB for 30 min. B, KHB for 30 min and 1 μM PMA for 30 min. C, KHB for 30 min and 10 nM VP for 30 min.
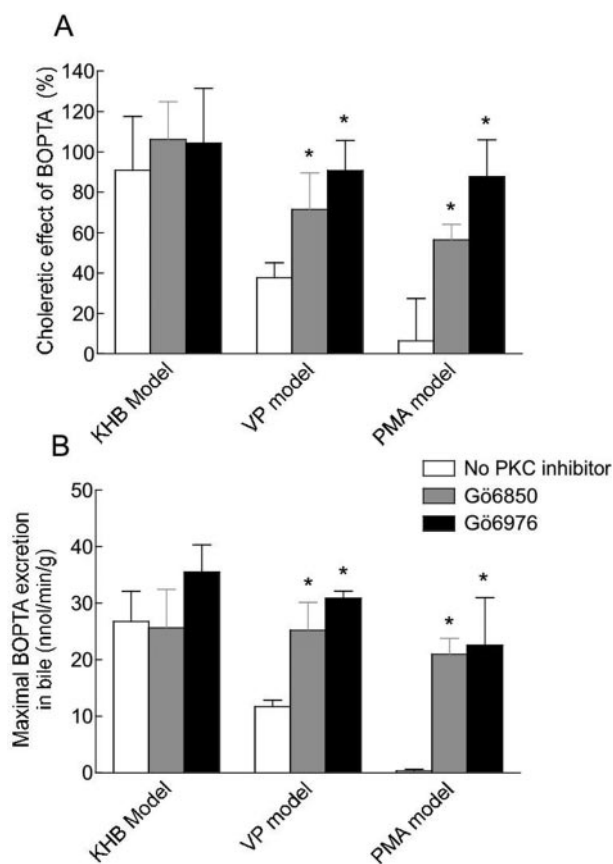
Fig. 5. Choleretic effect of BOPTA (%) (A) and maximal BOPTA bile excretion (B) during the perfusion of 200 μM Gd-BOPTA (from 45 to 75 min). In the KHB model, livers were preperfused with KHB, KHB + 1 μM Gö6850, or KHB + 1 μM Gö6976 (from 15 to 45 min) before BOPTA perfusion. In the VP model, livers were preperfused with KHB + 10 nM VP, KHB + 10 nM VP + 1 μM Gö6850, or KHB + 10 nM VP + 1 μM Gö6976 (from 15 to 45 min) before BOPTA perfusion. In the PMA model, livers were preperfused with KHB + 1 μM PMA, KHB + 1 μM PMA + 1 μM Gö6850, or KHB + 1 μM PMA + 1 μM Gö6976 (from 15 to 45 min) before BOPTA perfusion.

ium ethoxybenzyl diethylenetriaminepentaacetic acid in Oatp$_1$ cRNA-injected *X. laevis* oocytes is saturable with a K_m of 3.3 mM and inhibited by BSP, taurocholate, rifamycin, and rifampicin (Van Montfoort et al., 1999). The mouse Oatp$_1$ exhibited the same substrate specificity as the rat Oatp$_1$ (Hagenbuch et al., 2000).

The fact that the maximal HRP bile excretion was delayed compared with the maximal BOPTA bile excretion (Fig. 2) suggests that intracellular transport of BOPTA is mediated by cytoplasmic proteins rather than by a vesicular transport. Mrp$_2$ mediates the bile excretion of BOPTA, because in TR$^{-/-}$ rats, no BOPTA was measured in bile samples (data not shown). In vivo, bile excretion of BOPTA is also abolished in mutant TR$^{-/-}$ rats (de Haën et al., 1996). Bile excretion is 3% in TR$^{-/-}$ rats, whereas the excretion is 55% in wild-type rats. Other authors also showed that organic anions such as enalapril (Liu et al., 2006) and 5-(and 6)-carboxy-2′,7′-dichlorofluorescein (Chandra et al., 2005) are excreted via Mrp$_2$ because no organic anion is found in bile samples collected from rats without Mrp$_2$. Moreover, considering that biliary BOPTA excretion is maximal at 20 min after the start of BOPTA perfusion and constant thereafter (Fig. 1, BOPTA)

and that BOPTA accumulation in the liver is maximal at the end of BOPTA perfusion (Fig. 7), bile excretion through Mrp$_2$ is likely to limit BOPTA transport in normal livers.

Although BOPTA k_{uptake} was slightly lower in TR$^{-/-}$ rats (0.7 ± 0.3 min^{-1}) than in control rats (1.3 ± 0.3 min^{-1}), hepatic accumulation of BOPTA was higher in rats lacking Mrp$_2$ than in normal rats (Fig. 3D). During the rinse period after BOPTA perfusion, BOPTA remained trapped within hepatocytes without return back to the perfusate; the radioactivity measured in perfusate during this rinse period was similarly low in normal and TR$^{-/-}$ rats (0.522 ± 0.08 μmol in normal rats versus 0.601 ± 0.173 μmol in TR$^{-/-}$ rats). The small initial decrease in BOPTA concentration during the rinse period corresponded to the washout of the extracellular space by KHB perfusion. In contrast to the nonmetabolized probe substrate, 5- (and 6)-carboxy-2′,7′-dichlorofluorescein (Chandra et al., 2005), which can return to sinusoids through basolateral transporters (Mrp$_3$) in TR$^{-/-}$ livers, BOPTA did not exit through Mrp$_3$.

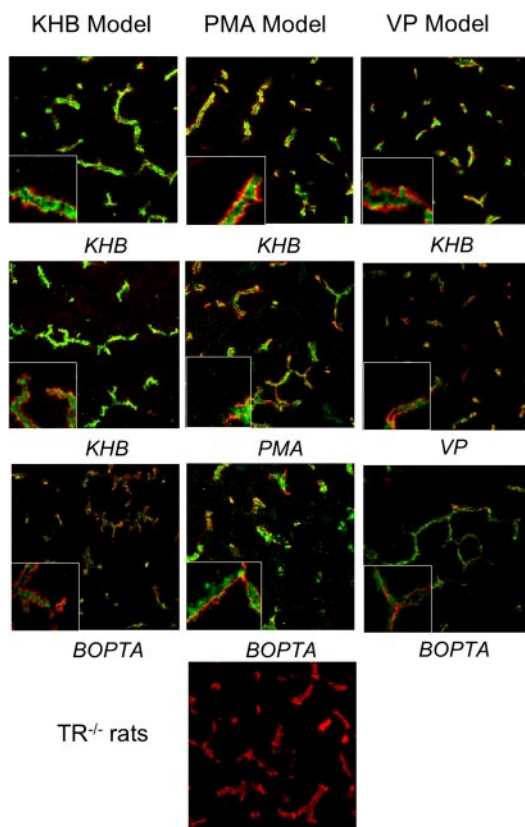**BOPTA Is a Choleretic Organic Anion without Anticholestatic Properties.** BOPTA bile excretion was associ-

Fig. 6. Subcellular localization of Mrp$_2$ immunofluorescence in the KHB model (livers are perfused with KHB during the entire protocol), the PMA model (livers are perfused with the subsequent conditions: KHB, PMA, and BOPTA), or the VP model (livers are perfused with the subsequent conditions: KHB, VP, and BOPTA). VP (10 nM), BOPTA (200 μM), PMA (1 μM). In the KHB model, virtually all Mrp$_2$ immunostaining (green) was confined to the space lined by the two rows of tight junctions stained by the anti-ZO-1 antibody (red), suggesting that Mrp$_2$ was localized within canalicular membranes. In the PMA and VP models, amount of Mrp$_2$ was found aside the tight junctions in the immediate vicinity of the canaliculi (Mrp$_2$ retrieval from the membrane). No Mrp$_2$ membrane reinsertion was observed during the Gd-BOPTA perfusion (see insets). No green staining was observed in rats without Mrp$_2$ (TR$^{-/-}$ rats).

TABLE 1
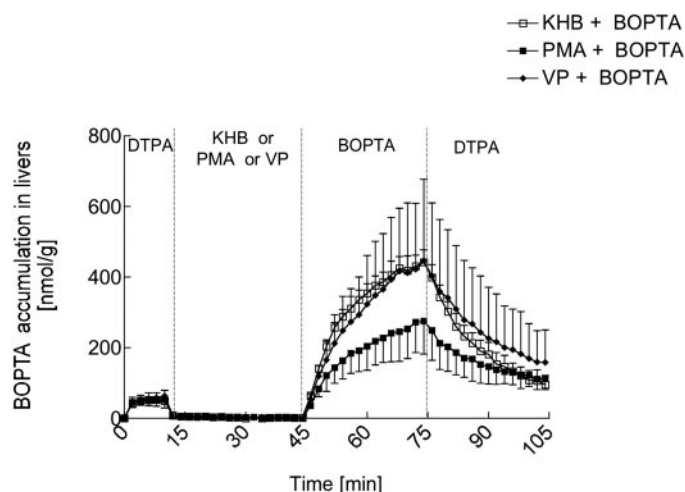Estimated uptake (k_{uptake}) and bile excretion ($k_{excretion}$) of Gd-BOPTA in entire livers
Values are means ± S.D. Means are compared by a one-way ANOVA and Dunnett test for multiple comparisons.

Models and Perfusion Solutions	k_{uptake}	$k_{excretion}$
	min^{-1}	
Control		
KHB	1.3 ± 0.3	0.11 ± 0.05
PMA		
KHB	0.4 ± 0.2*	0*
KHB + Gö6850	1.0 ± 0.2	0.07 ± 0.01
KHB + Gö6976	1.4 ± 0.1	0.07 ± 0.03
VP		
KHB	0.6 ± 0.1*	0.05 ± 0.01*
KHB + Gö6850	1.0 ± 0.4	0.11 ± 0.03
KHB + Gö6976	1.1 ± 0.2	0.08 ± 0.01
TR$^-$		
KHB	0.7 ± 0.3*	0*

* $P < 0.05$ vs. control.

Fig. 7. Gd-BOPTA accumulation in livers [nanomoles per gram] measured by a gamma scintillation probe placed 1 cm above the liver. Livers were perfused with the following solutions: KHB + Gd-DTPA (200 μM, 10 min); KHB, KHB + 1 μM PMA, or KHB + 10 nM VP for 30 min; KHB + Gd-BOPTA for 30 min; KHB for 30 min. Gd-DTPA, extracellular contrast agent that does not enter into hepatocytes.

ated with an increased bile flow as previously showed by de Haën et al. (1995). In contrast, when PKCα was activated by PMA, bile flow importantly decreased and subsequent BOPTA perfusion was unable to restore bile flow. Hepatic PMA perfusion was associated with the translocation of PKCα to cellular membranes (Fig. 4) and the endocytic retrieval of Mrp$_2$ from the canalicular membranes (Fig. 6). Subsequent perfusion with BOPTA was unable to reinsert Mrp$_2$ on the canalicular membrane. We hypothesized that phosphorylation of Mrp$_2$ by PKCα is responsible for the endocytic retrieval of the canalicular transporters preventing BOPTA from being excreted into bile in the PMA model. However, this hypothesis has to be questioned, because Beuers et al. (2001) showed that tauroursodeoxycholic acid inserts Mrp$_2$ in the canalicular membrane through a PKCα-dependent mechanism. The fact that Mrp$_2$ phosphorylation may either insert Mrp$_2$, as demonstrated in the study by Beuers et al. (2001), or retrieve the canalicular transporter, as observed in our study, remains puzzling.

Moreover, phosphorylation of Oatps by PKCα is likely to decrease BOPTA uptake into hepatocytes. When oocytes are incubated with PMA, E3S uptake is prevented (Fig. 3A). As previously shown by Guo and Klaassen (2001), PMA prevents the uptake of E3S, and PMA phosphorylates the Oatps with a loss of function. In oocytes incubated with BOPTA, however, we were unable to demonstrate a similar effect, probably because Oatp affinity for BOPTA is lower than the affinity of E$_3$S. In whole livers, BOPTA hepatic uptake estimated by k_{uptake} (Table 1) was significantly decreased by PMA. Consequently, the decreased BOPTA accumulation in the PMA model (Fig. 7) results from low uptake and absence of bile excretion. We were surprised to find that the return to perfusate was higher in the PMA model (1.11 ± 0.6 μmol) than in TR$^{-/-}$ rats (0.601 ± 0.173 μmol). Tiny hepatic injury by PMA cannot be excluded.

Endogenous PKCα activation through the signaling pathway down the sinusoidal V$_1$ receptors had no consequence on basal bile flow but decreased BOPTA bile excretion and consequently the choleretic effect of BOPTA. PKCα activation could not be evidenced by protein translocation, but Mrp$_2$ retrieval was observed (Fig. 6). Because the concomitant perfusion of VP and PKCα inhibitors prevented the decreased BOPTA bile excretion and restored the choleretic effect of the organic anion, we can conclude that the effects of VP on hepatic transporters were mediated by the PKCα activation. However, the effects of VP were less severe than those observed with PMA. When PKC activation by VP modulates both Oatps and Mrp$_2$ function in such a way that BOPTA entry and exit are similarly decreased (−54% and −55%, respectively), concentrations of organic anions within hepatocytes remain unaltered compared with livers perfused with KHB solution.

In summary, our results highlight that simultaneous analysis of the function of both sinusoidal and canalicular transporters is crucial to determine the concentration of organic anions within hepatocytes.

Acknowledgments

References

Beuers U, Bilzer M, Chittattu A, Kullak-Ublick GA, Keppler D, Paumgartner G, and Dombrowski F (2001) Tauroursodeoxycholic acid inserts the apical conjugate export pump, Mrp2, into canalicular membranes and stimulates organic anion secretion by protein kinase C−dependent mechanisms in cholestatic rat liver. *Hepatology* **33:**1206–1216.

Beuers U, Nathanson MH, Isales CM, and Boyer JL (1993) Tauroursodeoxycholic acid stimulates hepatocellular exocytosis and mobilizes extracellular Ca++ mechanisms defective in cholestasis. *J Clin Investig* **92:**2984–2993.

Chandra P, Johnson BM, Zhang P, Pollack GM, and Brouwer KL (2005) Modulation of hepatic canalicular or basolateral transport proteins alters hepatobiliary disposition of a model organic anion in the isolated perfused rat liver. *Drug Metab Dispos* **33:**1238–1243.

Cui Y, Konig J, Nies AT, Pfannschmidt M, Hergt M, Franke WW, Alt W, Moll R, and Keppler D (2003) Detection of the human organic anion transporters SLC21A6 (OATP2) and SLC21A8 (OATP8) in liver and hepatocellular carcinoma. *Lab Investig* **83:**527–538.

de Haën C, Lorusso V, Luzzani F, and Tirone P (1995) Hepatic transport of the magnetic resonance imaging contrast agent gadobenate dimeglumine in the rat. *Acad Radiol* **2:**232–238.

de Haën C, Lorusso V, and Tirone P (1996) Hepatic transport of gadobenate dimeglumine in TR-rats. *Acad Radiol* **3:**S454–S454.

Grazioli L, Morana G, Federle MP, Brancatelli G, Testoni M, Kirchin MA, Menni K, Olivetti L, Nicoli N, and Procacci C (2001) Focal nodular hyperplasia: morphologic and functional information from MR imaging with gadobenate dimeglumine. *Radiology* **221:**731–739.

Guo GL and Klaassen CD (2001) Protein kinase C suppresses rat organic anion transporting polypeptide 1- and 2-mediated uptake. *J Pharmacol Exp Ther* **299:**551–557.

Hagenbuch B, Adler ID, and Schmid TE (2000) Molecular cloning and functional characterization of the mouse organic-anion-transporting polypeptide 1 (Oatp1) and mapping of the gene to chromosome X. *Biochem J* **345:**115–120.

Hagenbuch B, Lübbert H, Stieger B, and Meier PJ (1990) Expression of the hepatic Na$^+$/bile acid cotransporter in *Xenopus laevis* oocytes. *J Biol Chem* **265:**5357–5360.

Hagenbuch B and Meier PJ (2003) The superfamily of organic anion transporting polypeptides. *Biochim Biophys Acta* **1609:**1–18.

Hoffmaster KA, Zamek-Gliszczynski MJ, Pollack GM, and Brouwer KL (2004) Hepatobiliary disposition of the metabolically stable opioid peptide [D-Pen², D-Pen⁵]-enkephalin (DPDPE): pharmacokinetic consequences of the interplay between multiple transport systems. *J Pharmacol Exp Ther* **311:**1203–1210.

Hsiang B, Zhu Y, Wang Z, Wu Y, Sasseville V, Yang W-P, and Kirchgessner TG (1999) A novel human hepatic organic anion transporting polypeptide (OATP2). Identification of a liver-specific human organic anion transporting polypeptide and identification of rat and human hydroxymethylglutaryl-CoA reductase inhibitor transporters. *J Biol Chem* **274:**37161–37168.

Keppler D and König J (1997) Expression and localization of the conjugate export pump encoded by the MRP2 (cMRP/cMOAT) gene in liver. *FASEB J* **11:**509–516.

König J, Cui Y, Nies AT, and Keppler D (2000) A novel human organic anion transporting polypeptide localized to the basolateral hepatocyte membrane. *Am J Physiol* **278:**G156–G164.

Kullak-Ublick GA, Beuers U, and Paumgartner G (2000) Hepatobiliary transport. *J Hepatol* **32:Suppl** 1:3–18.

Kullak-Ublick GA, Ismair MG, Stieger B, Landmann L, Huber R, Pizzagalli F, Fattinger K, Meier PJ, and Hagenbuch B (2001) Organic anion-transporting polypeptide B (OATP-B) and its functional comparison with three other OATPs of human liver. *Gastroenterology* **120:**525–533.

Liu L, Cui Y, Chung AY, Shitara Y, Sugiyama Y, Keppler D, and Pang KS (2006) Vectorial transport of enalapril by Oatp1a1/Mrp2 and OATP1B1 and OATP1B3/MRP2 in rat and human livers. *J Pharmacol Exp Ther* **318:**395–402.

Manfredi R, Maresca G, Baron RL, de Franco A, de Gaetano AM, Cotroneo AR, Pirovano G, Spinazzi A, and Marano P (1998) Gadobenate dimeglumine (BOPTA) enhanced MR imaging: patterns of enhancement in normal liver and cirrhosis. *J Magn Reson Imaging* **8:**862–867.

Matsushima S, Maeda K, Kondo C, Hirano M, Sasaki M, Suzuki H, and Sugiyama Y (2005) Identification of the hepatic efflux transporters of organic anions using double-transfected Madin-Darby canine kidney II cells expressing human organic anion-transporting polypeptide 1B1 (OATP1B1)/multidrug resistance-associated protein 2, OATP1B1/multidrug resistance 1, and OATP1B1/breast cancer resistance protein. *J Pharmacol Exp Ther* **314:**1059–1067.

Meier PJ, Eckhardt U, Schroeder A, Hagenbuch B, and Stieger B (1997) Substrate specificity of sinusoidal bile acid and organic anion uptake systems in rat and human liver. *Hepatology* **26:**1667–1677.

Noé B, Hagenbuch B, Stieger B, and Meier PJ (1997) Isolation of a multispecific organic anion and cardiac glycoside transporter from rat brain. *Proc Natl Acad Sci USA* **94:**10346–11050.

Pastor CM, Planchamp C, Pochon S, Lorusso V, Montet X, Mayer J, Terrier F, and Vallée J-P (2003) Kinetics of gadobenate dimeglumine in isolated perfused rat liver: MR imaging evaluation. *Radiology* **229:**119–125.

Pastor CM, Wiliams D, Yoneyama T, Hatakeyama K, Singleton S, Naylor E, and Billiar TR (1996) Competition for tetrahydrobiopterin between phenylalanine hydroxylase and nitric oxide synthase in rat liver. *J Biol Chem* **271:**24534–24538.

Patel NJ, Zamek-Gliszczynski MJ, Zhang P, Han YH, Jansen PL, Meier PJ, Stieger B, and Brouwer KL (2003) Phenobarbital alters hepatic Mrp2 function by direct and indirect interactions. *Mol Pharmacol* **64:**154–159.

Planchamp C, Beyer GJ, Slosman DO, F Terrier F, and Pastor CM (2005a) Direct evidence of the temperature dependence of Gd-BOPTA transport in the intact liver. *Appl Radiat Isot* **62:**943–949.

Planchamp C, Gex-Fabry M, Dornier C, Quadri R, Reist M, Ivancevic MK, Vallée JP,

Pochon S, Terrier F, Balant L, et al. (2004) Gd-BOPTA transport into rat hepatocytes: pharmacokinetic analysis of magnetic resonance images using a hollow fiber bioreactor. *Investig Radiol* **39:**506–515.

Planchamp C, Pastor CM, Balant L, Becker CD, Terrier F, and Gex-Fabry M (2005b) Quantification of Gd-BOPTA uptake and biliary excretion from dynamic MRI in rat livers: model validation with ^{153}Gd-BOPTA. *Investig Radiol* **40:**705–714.

Roelofsen H, Ottenhoff R, Oude Elferink RP, and Jansen PL (1991) Hepatocanalicular organic-anion transport is regulated by protein kinase C. *Biochem J* **278:**637–641.

Sasaki M, Suzuki H, Aoki J, Ito K, Meier PJ, and Sugiyama Y (2004) Prediction of in vivo biliary clearance from the in vitro transcellular transport of organic anions across a double-transfected Madin-Darby canine kidney II monolayer expressing both rat organic anion transporting polypeptide 4 and multidrug resistance associated protein 2. *Mol Pharmacol* **66:**450–459.

Van Montfoort JE, Stieger B, Meijer DKF, Weinmann H-J, Meier PJ, and Fattinger KE (1999) Hepatic uptake of the magnetic resonance imaging contrast agent gadoxetate by organic anion transporting polypeptide Oatp1. *J Pharmacol Exp Ther* **290:**153–157.

Address correspondence to: Dr. Catherine M. Pastor, Laboratoire de Physiopathologie Hépatique et Imagerie Moléculaire, Hôpitaux Universitaires de Genève, Rue Micheli-du-Crest, 24, 1205 Geneva, Switzerland. E-mail: catherine.pastor@hcuge.ch